

## Selective Recognition of G-Quadruplex Telomeric DNA by a Bis(quinacridine) Macrocycle

Marie-Paule Teulade-Fichou,<sup>\*,†</sup> Carolina Carrasco,<sup>‡</sup> Lionel Guittat,<sup>§</sup> Christian Bailly,<sup>‡</sup> Patrizia Alberti,<sup>§</sup> Jean-Louis Mergny,<sup>§</sup> Arnaud David,<sup>†</sup> Jean-Marie Lehn,<sup>†</sup> and W. David Wilson<sup>\*,||</sup>

*Contribution from the Laboratoire de Chimie des Interactions Moléculaires, Collège de France, CNRS UPR 285, 11 place Marcelin Berthelot, 75005 Paris, France, INSERM U524 et Laboratoire de Pharmacologie Antitumorale du Centre Oscar Lambret, IRCL, Place de Verdun, 59045 Lille, France, Laboratoire de Biophysique, Museum National d'Histoire Naturelle INSERM U565, CNRS UMR 8646, 43 rue Cuvier, 75231 Paris Cedex 05, France, and Department of Chemistry, Georgia State University, Atlanta, Georgia 30303*

Received October 23, 2002; E-mail: chewdw@panther.gsu.edu

**Abstract:** The interaction of G-quadruplex DNA with the macrocyclic compound BOQ1, which possesses two dibenzophenanthroline (quinacridine) subunits, has been investigated by a variety of methods. The oligonucleotide 5'-A(GGGT<sub>2</sub>A)<sub>3</sub>G<sub>3</sub>, which mimics the human telomeric repeat sequence and forms an intramolecular quadruplex, was used as one model system. Equilibrium binding constants measured by biosensor surface plasmon resonance (SPR) methods indicate a high affinity of the macrocycle for the quadruplex conformation ( $K > 1 \times 10^7 \text{ M}^{-1}$ ) with two equivalent binding sites. The affinity of BOQ1 for DNA duplexes is at least 1 order of magnitude lower. In addition, the macrocycle is more selective than the monomeric control compound (MOQ2), which is not able to discriminate between the two DNA structures ( $K_{\text{duplex}} \approx K_{\text{quadruplex}} \approx 10^6 \text{ M}^{-1}$ ). Strong binding of BOQ1 to G4 DNA sequences was confirmed by fluorometric titrations with a tetraplex-forming oligonucleotide. Competition dialysis experiments with a panel of different DNA structures, from single strands to quadruplexes, clearly established the quadruplex binding specificity of BOQ1. Fluorescence resonance energy transfer (FRET)  $T_m$  experiments with a doubly labeled oligonucleotide also revealed a strong stabilization of the G4 conformation in the presence of BOQ1 ( $\Delta T_m = +28 \text{ }^\circ\text{C}$ ). This  $\Delta T_m$  value is one of the highest values measured for a G-quadruplex ligand and is significantly higher than observed for the monomer control compounds ( $\Delta T_m = +10\text{--}12 \text{ }^\circ\text{C}$ ). Gel mobility shift assays indicated that the macrocycle efficiently induces the formation of G-tetraplexes. Strong inhibition of telomerase was observed in the submicromolar range ( $\text{IC}_{50} = 0.13 \text{ } \mu\text{M}$ ). These results indicate that macrocycles represent an exciting new development opportunity for targeting DNA quadruplexes.

### Introduction

Although the structural complexity of RNA has been recognized from the early studies of tRNA to the recent structure of the ribosome, there is increasing understanding of the importance of structural polymorphism of DNA. Sequence-dependent structural flexibility of DNA and its importance for DNA function and specific interactions are now clearly documented.<sup>1</sup> The structural variations of chromosomal telomeres present a more recent example of DNA polymorphism that is critical for biological function.<sup>2</sup> The study of telomeres and the telomerase enzyme that maintains their length has acquired importance through the discovery of telomerase activity in most types of

cancer cells.<sup>3</sup> The enzyme is normally inactive in somatic cells and, thus, presents a new and potentially very specific therapeutic target for drug development.<sup>4</sup> Compounds for targeting the reverse transcriptase activity of the enzyme,<sup>5</sup> its RNA component,<sup>6</sup> or the DNA substrate<sup>7</sup> have been reported. Te-

<sup>†</sup> Collège de France.

<sup>‡</sup> Laboratoire de Pharmacologie Antitumorale du Centre Oscar Lambret.

<sup>§</sup> Museum National d'Histoire Naturelle.

<sup>||</sup> Georgia State University.

(1) (a) Lebrun, A.; Lavery, R. *Curr. Opin. Struct. Biol.* **1997**, *7*, 348–354. (b) Gilbert, D. E.; Feigon, J. *Curr. Opin. Struct. Biol.* **1999**, *9*, 305–314. (c) Williams, L. D.; Maher, L. J. *Annu. Rev. Biophys. Biomol. Struct.* **2000**, *29*, 497–521.

(2) (a) Wang, Y.; Patel, D. J. *Structure* **1993**, *1*, 263–282. (b) Greider, C. W. *Annu. Rev. Biochem.* **1996**, *65*, 337–365. (c) McEachern, M. J.; Krauskopf, A.; Blackburn, E. H. *Annu. Rev. Genet.* **2000**, *34*, 331–358. (d) Munoz-Jordan, J. L.; Cross, G. A.; de Lange, T.; Griffith, J. D. *EMBO J.* **2001**, *20*, 579–588. (e) Ren J.; Qu X.; Trent J. O.; Chaires, J. B. *Nucleic Acids Res.* **2002**, *30*, 2307–2315. (f) Parkinson, G. N.; Lee, M. P.; Neidle, S. *Nature* **2002**, *417*, 876–880.

(3) (a) Kim, N. W.; Piatyszek, M. A.; Prowse, K. R.; Harley, C. B.; West, M. D.; Ho, P. L. C.; Coviello, G. M.; Wright, W. E.; Weinrich, S. L.; Shay, J. W. *Science* **1994**, *266*, 2011–2015. (b) Hahn, W. C.; Stewart, S. A.; Brooks, M. W.; Shoshana, G. Y.; Eaton, E.; Kurachi, A.; Beijersbergen, R. L.; Knoll, J. H. M.; Meyerson, M.; Weinberg, R. A. *Nat. Med.* **1999**, *5*, 1164–1170. (c) Hanahan, D.; Weinberg, R. A. *Cell* **2000**, *100*, 57–70. (d) Greider, C. W. *Harvey Lect.* **2001**, *96*, 33–50. (e) Granger, M. P.; Wright, W. E.; Shay, J. W. *Crit. Rev. Oncol. Hematol.* **2002**, *41*, 29–40.

(4) (a) Herbert, B. S.; Pitts, A. E.; Baker, S. I.; Hamilton, S. E.; Wright, W. E.; Shay, J. W.; Corey, D. R. *Proc. Natl. Acad. Sci. U.S.A.* **1999**, *96*, 14276–14281. (b) Mergny, J.-L.; Riou, J.-F.; Mailliet, P.; Teulade-Fichou, M.-P.; Gilson, E. *Nucleic Acids Res.* **2002**, *30*, 839–865. (c) McCaul, J. A.; Gordon, K. E.; Clark, L. J.; Parkinson, E. K. *Lancet Oncol.* **2002**, *3*, 280–288.

lomerase activity is also present in a number of disease-causing parasitic microorganisms,<sup>8</sup> and the enzyme offers a possible site for the targeting of these organisms that causes such serious and widespread diseases for which few drugs are available.

The telomere DNA consists of a single-stranded G-rich 3'-terminal sequence, (GGTTAG)<sub>n</sub> in humans, and a duplex region where the G-rich sequence base-pairs with a Watson-Crick complementary C-rich strand and connects with the chromosomal duplex. In the nonreplicative state the single strand can invade the telomere duplex to form a t-loop structure that appears to be important in stabilizing the ends of chromosomes.<sup>9</sup> For telomerase activity this t-loop must dissociate to present the G-rich single strand to the enzyme. A novel idea for anticancer drug design is to use small molecules that bind to G4 tetraplexes to drive this single strand into a stable tetraplex that can inhibit the telomerase enzyme.<sup>10</sup> Several classes of small molecules that selectively bind to DNA tetraplexes and inhibit telomerase have been described.<sup>7,10</sup> There are also G-rich sequences in the transcription control regions of important oncogenes.<sup>11</sup> Targeting of G4 structures has taken on increased importance on the basis of recent evidence that the transcriptional activity of these oncogenes can be modulated through small molecule induction and/or stabilization of G4 tetraplexes.<sup>11a</sup> Given the wide distribution of guanine-rich sequences in chromosomal DNA<sup>12</sup> and the possible existence of four-stranded

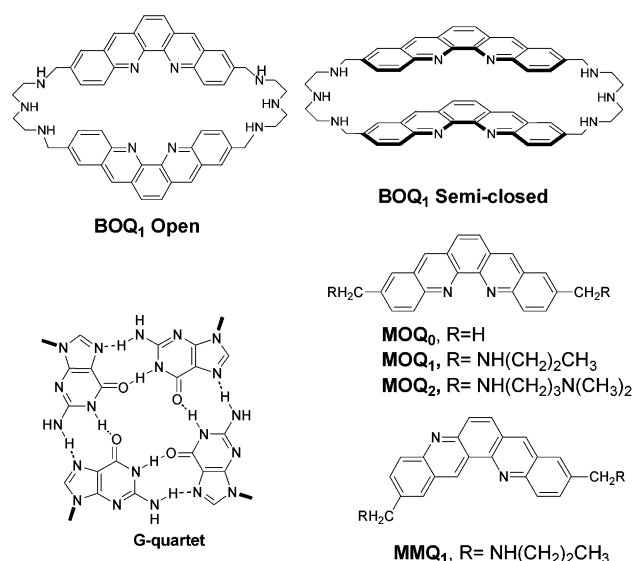


**Figure 1.** Chemical structures of the macrocycle BOQ<sub>1</sub>, in the open and semiclosed conformations, and the monomer compounds are shown. A G-quartet is also shown for an approximate size reference.

RNAs,<sup>13</sup> it is reasonable to expect that further regulatory functions of nucleic acids tetraplexes will be found soon.<sup>14</sup>

General features of molecules that bind to G4 tetraplexes include a large flat aromatic surface and cationic charges.<sup>7,10</sup> These compounds are generally similar to intercalators or are derivatives of well-known intercalators.<sup>10</sup> Such a molecular motif can stack with the terminal G quartets and form specific electrostatic contacts. This binding mode was initially inferred from steric and geometric considerations and has been supported by NMR and modeling studies.<sup>10,15</sup> Terminal stacking, thus, constitutes a "consensus binding model" that is also compatible with the different forms of quadruplexes.<sup>2,12</sup> However, many compounds studied so far that adopt the terminal stacking mode suffer from poor or insufficient preference for quadruplexes over duplexes. The discovery of new G4-specific compounds is thus of utmost importance for a more comprehensive understanding of the biological implications of these structures and for designing new drugs with enhanced activity and minimized undesired toxicity.

In our search for promising compounds for selective targeting of G4 tetraplexes, our attention was drawn to cationic macrocycles (Figure 1) for several reasons. Cyclobisintercaland compounds are a family of macrocyclic compounds constituted of two intercalative-type moieties bridged by polyammonium linkers and were originally designed on the basis of supramolecular concepts for molecular recognition of nucleotides.<sup>16,17</sup>

- (5) (a) Fletcher, T. M.; Salazar, M.; Chen, S. F. *Biochemistry* **1996**, *35*, 15611–15617. (b) Gomez, D. E.; Tejera, A. M.; Olivero, O. A. *Biochem. Biophys. Res. Commun.* **1998**, *246*, 107–110. (c) Murakami, J.; Nagai, N.; Shigemasa, K.; Ohama, K. *Eur. J. Cancer* **1999**, *35*, 1027–1034. (d) Fletcher, T. M.; Cathers, B. E.; Ravikumar, K. S.; Mamiya, B. M.; Kerwin, S. M. *Bioorg. Chem.* **2001**, *29*, 36–55.
- (6) (a) Pitts, A. E.; Corey, D. R. *Proc. Natl. Acad. Sci. U.S.A.* **1998**, *95*, 11549–11554. (b) Pruzan, R.; Pongracz, K.; Gietzen, K.; Wallweber, G.; Gryaznov, S. *Nucleic Acids Res.* **2002**, *30*, 559–568.
- (7) (a) Raymond, E.; Soria, J.; Izbička, E.; Boussin, F.; Hurley, L. H.; Von Hoff, D. D. *Invest. New Drugs* **2000**, *18*, 123–137. (b) Kerwin, S. M. *Curr. Pharm. Des.* **2000**, *6*, 441–471. (c) Kelland, L. R. *Anticancer Drugs* **2000**, *11*, 503–513. (d) Sun, D.; Hurley, L. H. *Methods Enzymol.* **2001**, *340*, 573–592. (e) Perry, P. J.; Arnold, J. R. P.; Jenkins, T. C. *Expert Opin. Investig. Drugs* **2001**, *10*, 2141–2156. (f) Neidle, S.; Parkinson, G. *Nat. Drug Discov.* **2002**, *1*, 383–393. (g) Rezler, E. M.; Bearss, D. J.; Hurley, L. H. *Curr. Opin. Pharmacol.* **2002**, *2*, 415–423.
- (8) (a) Cano, M.; Dungan, J.; Agabian, N.; Blackburn, E. H. *Proc. Natl. Acad. Sci. U.S.A.* **1999**, *96*, 3616–3621. (b) Bottius, E.; Bakhsis, N.; Scherf, A. *Mol. Cell. Biol.* **1998**, *18*, 919–925.
- (9) Griffith, J. D.; Comeau, L.; Rosenfield, S. D.; Stansel, R. M.; Bianchi, A.; Moss, H.; de Lange, T. *Cell* **1999**, *97*, 503–514.
- (10) (a) Sun, D.; Thompson, B.; Cathers, B. E.; Salazar, M.; Kerwin, S. M.; Trent, J. O.; Jenkins, T. C.; Neidle, S.; Hurley, L. H. *J. Med. Chem.* **1997**, *40*, 2113–2116. (b) Perry, P. J.; Gowan, S. M.; Reszka, A. P.; Polucci, P.; Jenkins, T. C.; Kelland, L. R.; Neidle, S. *J. Med. Chem.* **1998**, *41*, 3253–3260. (c) Mergny, J.-L.; Hélène, C. *Nat. Med.* **1998**, *4*, 1366–1367. (d) Harrison, R. J.; Gowan, S.; Kelland, L. R.; Neidle, S. *Bioorg. Med. Chem. Lett.* **1999**, *9*, 2463–2468. (e) Han, H.; Cliff, C. L.; Hurley, L. H. *Biochemistry* **1999**, *38*, 6981–6986. (f) Hurley, L. H.; Wheelhouse, R. T.; Sun, D.; Kerwin, S. M.; Salazar, M.; Fedoroff, O. Y.; Han, F. X.; Han, H.; Izbička, E.; Von Hoff, D. D. *Pharm. Ther.* **2000**, *85*, 141–158. (g) Perry, P. J.; Jenkins, T. C. *Med. Chem.* **2001**, *1*, 1–41. (h) Han, H.; Langley, D.; Rangan, A.; Hurley, L. H. *J. Am. Chem. Soc.* **2001**, *123*, 8902–8913. (i) Koepfel, F.; Riou, J. F.; Laoui, A.; Mailliet, P.; Arimondo, P. B.; Petitgenet, D. O.; Hélène, C.; Mergny, J. L. *Nucleic Acids Res.* **2001**, *29*, 1087–1096. (j) Alberti, P.; Ren, J.; Teulade-Fichou, M. P.; Guittat, L.; Riou, J. F.; Chaires, J.; Hélène, C.; Vigneron, J. P.; Lehn, J. M.; Mergny, J. L. *J. Biomol. Struct. Dyn.* **2001**, *19*, 505–513. (k) Kerwin, S. M.; Sun, D.; Kern, J. T.; Rangan, A.; Thomas, P. W. *Bioorg. Med. Chem. Lett.* **2001**, *11*, 2411–2414. (l) Gavathiotis, E.; Heald, R. A.; Stevens, M. F. G.; Searle, M. S. *Angew. Chem., Int. Ed.* **2001**, *40*, 4749–4751. (m) Read, M.; Harrison, R. J.; Romagnoli, B.; Taniou, F. A.; Gowan, S. H.; Reszka, A. P.; Wilson, W. D.; Kelland, L. R.; Neidle, S. *Proc. Natl. Acad. Sci. U.S.A.* **2001**, *98*, 4844–4849. (n) Tuntiwechapakul, W.; Jeong, T. L.; Salazar, M. *J. Am. Chem. Soc.* **2001**, *123*, 5606–5607. (o) Kim, M. Y.; Vankayalapati, H.; Shin-Ya, K.; Wierzbza, K.; Hurley, L. H. *J. Am. Chem. Soc.* **2002**, *124*, 2098–2099. (p) Kern, J. T.; Thomas, P. W.; Kerwin, S. M. *Biochemistry* **2002**, *41*, 11379–89; and references cited in the above.
- (11) (a) Rangan, A.; Siddiqui-Jain, A.; Grand, C. L.; Bearss, D. J.; Hurley, L. H. *Proc. Natl. Acad. Sci. U.S.A.* **2002**, *99*, 11593–11598. (b) Fedoroff, O. Y.; Hurley, L. H. *J. Biol. Chem.* **2001**, *276*, 4640–4646. (c) Simonsson, T.; Pecinka, P.; Kubista, M. *Nucleic Acids Res.* **1998**, *26*, 1167–1172.
- (12) (a) Arthanari, H.; Bolton, P. H. *Chem. Biol.* **2001**, *8*, 221–230. (b) Keniry, M. A. *Biopolymers* **2001**, *56*, 123–146.
- (13) (a) Kim, J.; Cheong, C.; Moore, P. B. *Nature* **1991**, *351*, 331–332. (b) Deng, J.; Xiong, Y.; Sundaralingam, M. *Proc. Natl. Acad. Sci. U.S.A.* **2001**, *98*, 13665–13670. (c) Darnell, J. C.; Jensen, K. B.; Jin, P.; Brown, V.; Warren, S. T.; Darnell, R. B. *Cell* **2001**, *107*, 489–499. (d) Schaeffer, C.; Bardoni, B.; Mandel, J. L.; Ehresmann, B.; Ehresmann, C.; Moine, H. *EMBO J.* **2001**, *20*, 4803–4813.
- (14) Unrau, P.; Johnson, J. R. *J. Theor. Biol.* **1995**, *177*, 73–86.
- (15) (a) Mergny, J.-L.; Mailliet, P.; Lavelle, F.; Riou, J.-F.; Laoui, A.; Hélène, C. *Anti-Cancer Drug Des.* **1999**, *14*, 427–439. (b) Read, M. A.; Neidle, S. *Biochemistry* **2000**, *39*, 13422–13432. (c) Fedoroff, O. Y.; Salazar, M.; Han, H.; Chemeris, V. V.; Kerwin, S. M.; Hurley, L. H. *Biochemistry* **1998**, *37*, 12368–12375. (d) Han, F. X.; Wheelhouse, R. T.; Hurley, L. H. *J. Am. Chem. Soc.* **1999**, *121*, 3561–3570.
- (16) Baudoin, O.; Teulade-Fichou, M.-P.; Vigneron, J.-P.; Lehn, J.-M. *J. Org. Chem.* **1997**, *62*, 5458–5470.

BOQ1, which contains two large pentacyclic units (dibenzo[*b,j*]-1,10-phenanthroline, referred to as quinacridine) has shown the ability to selectively trap GG base pairs.<sup>17</sup> This property was attributed to the crescent-shaped and large surface of the quinacridine ring suitable for  $\pi$ -orbital overlap with two guanines paired by Hoogsteen hydrogen bonds.<sup>17,18</sup> Likewise, the propensity of the quinacridine motif to stack on large aromatic areas should in part contribute to the affinity for G-quadruplexes as observed for the members of the 2,10-disubstituted *m*-quinacridine series (dibenzo[*b,j*]-1,7-phenanthroline derivatives) recently reported.<sup>19</sup> Moreover, cyclobisintercalands display preferential binding to nucleic acids motifs that contain exposed bases such as hairpin loops.<sup>20,21</sup> This selective behavior is attributed to their cyclic framework that disfavors their insertion into a DNA double helix. Compound BOQ1 (Figure 1), which combines large subunits that are able to stack on a G quartet and a macrocyclic scaffold likely to have favorable groove/loop interactions (Figure 1), thus appeared to be a very promising potential candidate for binding to G-quadruplexes. This hypothesis was tested here with BOQ1 and four control monomers, shown in Figure 1. A broad panel of biophysical and biochemical techniques was applied to evaluate their interactions with telomere sequences and their effects on telomerase activity. We have found that BOQ1 has very strong binding with significant specificity for quadruplex over duplex interactions. This compound thus presents a new motif for the design of potential telomere-targeted anticancer drugs.

## Materials and Methods

**Compounds and Oligonucleotides.** The syntheses of dibenzophenanthrolines MMQ1, MOQ0–2, and BOQ1 have been described previously.<sup>16</sup> Oligodeoxynucleotide probes were synthesized by Eurogentec (Belgium). Purity was checked by gel electrophoresis. All concentrations were expressed in strand molarity with a nearest-neighbor approximation for the absorption coefficients of the unfolded species.<sup>22</sup> All polynucleotides were from Amersham–Pharmacia. F21T [5′G<sub>3</sub>(TTAG<sub>3</sub>)<sub>3</sub>] is a doubly fluorescently labeled 21-base-long oligomer that mimics the telomeric guanine-rich strand. Three 5′-biotin-labeled oligomers (Eurogentec, PAGE-purified) were used in surface plasmon resonance studies: the [AATT] duplex d(biotin-CGAATTCGTCCTCGAATTCG), the [CG]<sub>4</sub> duplex d(biotin-CGCGCGCTTTTCGCGCGCG) (hairpin loops underlined), and the G4 quadruplex d(biotin-[AG<sub>3</sub>(TTAG<sub>3</sub>)<sub>3</sub>]). Two oligonucleotides (Eurogentec, PAGE purified) were used for fluorometric titration: 22A, d[5′AG<sub>3</sub>(TTAG<sub>3</sub>)<sub>3</sub>], and the 17-bp duplex d(5′-ATCCAGTTCGTAGTAAC)/d(5′-GTTACTACGAACTGGAT).<sup>23</sup>

**Fluorescence Resonance Energy Transfer.** FRET can be used to probe the secondary structure of oligodeoxynucleotides mimicking repeats of the guanine-rich strand of vertebrate telomeres, provided a fluorescein molecule (donor) and a tetramethylrhodamine derivative (acceptor) are attached to the 5′ and 3′ ends of the oligonucleotide,

respectively. All FRET measurements with the F21T oligonucleotide were performed on a Spex Fluorolog DM1B instrument, with a bandwidth of 1.8 nm and 0.2- × 1-cm quartz cuvettes, containing 600  $\mu$ L of solution in a 0.1 M lithium chloride/10 mM sodium cacodylate buffer, pH 7.2. The experiments were performed with lithium ion to keep the  $T_m$  values of the complexes in the measurable range. The temperature of the circulating water bath was recorded at regular time intervals. All measurements were performed as previously described.<sup>24</sup>

**Immobilization of DNA and Surface Plasmon Resonance Binding.** Surface plasmon resonance (SPR) measurements were performed with a four-channel BIAcore 3000 optical biosensor system (Biacore Inc.) and streptavidin-coated sensor chips (Biacore SA-chip). Samples of biotin-labeled DNA oligomers were applied to flow cells in streptavidin-derivatized sensor chips as previously described.<sup>25</sup> Steady-state binding analysis was performed with multiple injections of different compound concentrations over the immobilized DNA surface at 25 °C. DNA binding experiments were performed in HBS-EP buffer (sterile filtered and degassed buffer obtained from BIAcore: 0.01 M HEPES, pH 7.4, 0.15 M NaCl, 3 mM EDTA, and 0.005% surfactant P20) supplemented with 0.2 M KCl. Compound solutions were prepared in filtered and degassed HBS-EP/KCl buffer by serial dilutions from stock solution and were injected from 7 mm plastic vials with pierceable plastic crimp caps (BIAcore Inc.). Buffer flow alone was sufficient to dissociate the DNA complexes.

The instrument response (RU) in the steady-state region is proportional to the amount of bound drug and was determined by linear averaging over a 80 s time span. The predicted maximum response per bound compound in the steady-state region (RU<sub>max</sub>) is determined from the DNA molecular weight, the amount of DNA on the flow cell, the compound molecular weight, and the refractive index gradient ratio of the compound and DNA, as previously described.<sup>26</sup> In most of the cases, the observed RU values at high concentrations are greater than RU<sub>max</sub>, pointing to more than one binding site in these DNA sequences. The number of binding sites was determined from Scatchard plots of RU/concentration vs RU plot by a linear regression analysis. The RU<sub>max</sub> value is required to convert the observed response (RU) to the standard binding parameter  $r$  (moles of drug bound/moles of DNA hairpin):

$$r = \text{RU}/\text{RU}_{\text{max}}$$

To obtain the affinity constants, the results from the steady-state region were fitted with a multiple equivalent-site model, and Kaleidagraph was used for nonlinear least-squares optimization of the binding parameters:

$$r = nKC_{\text{free}}/(1 + KC_{\text{free}})$$

where  $K$ , the microscopic binding constant, is one variable to fit;  $r$  represents the moles of bound compound per mole of DNA hairpin duplex;  $C_{\text{free}}$  is the concentration of the compound in equilibrium with the complex and is fixed by the concentration in the flow solution; and  $n$  is the number of compound binding sites on the DNA duplex and is the second variable to fit.

**Accelerated Assembly of G Quadruplexes.** The purified Tr2 (5′ TACAGATAGTTAGGGTTAGGGTTA) and Ox-1T (5′ ACTGTCTGCTACTTGATAGGGGTTTTGGGGGAATGTGA) oligodeoxynucleotides were 5′-end-labeled and used at a final strand concentration of 8  $\mu$ M. The solution was heated to 95 °C for 5 min in a TE buffer containing

- (17) Baudoin, O.; Gonnet, F.; Teulade-Fichou, M.-P.; Vigneron, J.-P.; Tabet, J.-C.; Lehn, J.-M. *Chem. Eur. J.* **1999**, *5*, 2762–2771.  
 (18) Baudoin, O. Ph.D. Thesis, University P&M Curie, Paris, France, 1998.  
 (19) Mergny, J.-L.; Lacroix, L.; Teulade-Fichou, M.-P.; Hounsou, C.; Guittat, L.; Hoarau, M.; Arimondo, P. B.; Vigneron, J.-P.; Lehn, J.-M.; Riou, J.-F.; Garestier, T.; Hélène, C. *Proc. Natl. Acad. Sci. U.S.A.* **2001**, *98*, 3062–3067.  
 (20) Slama-Schwok, A.; Teulade-Fichou, M.-P.; Vigneron, J.-P.; Taillandier, E.; Lehn, J.-M. *J. Am. Chem. Soc.* **1995**, *117*, 6822–6829.  
 (21) Blacker, A. J.; Teulade-Fichou, M.-P.; Vigneron, J.-P.; Fauquet, M.; Lehn, J.-M. *Bioorg. Med. Chem. Lett.* **1998**, *8*, 601–606.  
 (22) Cantor, C. R.; Warshaw, M. M.; Shapiro, H. *Biopolymers* **1970**, *9*, 1059–1077.  
 (23) Serva, S.; Weinhold, E.; Roberts, R. J.; Klimasauskas, S. *Nucleic Acids Res.* **1998**, *26*, 3473–3479.

- (24) Mergny, J.-L.; Maurizot, J. C. *ChemBioChem* **2001**, *2*, 124–132.  
 (25) (a) Wang, L.; Bailly, C.; Kumar, A.; Ding, D.; Bajic, M.; Boykin, D. W.; Wilson, W. D. *Proc. Natl. Acad. Sci. U.S.A.* **2000**, *97*, 12–16. (b) Wang, L.; Carrasco, C.; Kumar, A.; Stephens, C. E.; Bailly, C.; Boykin, D. W.; Wilson, W. D. *Biochemistry* **2001**, *40*, 2511–2521. (c) Mazur, S.; Taniou, F. A.; Ding, D.; Kumar, A.; Boykin, D. W.; Simpson, I. J.; Neidle, S.; Wilson, W. D. *J. Mol. Biol.* **2000**, *300*, 321–337. (d) Nguyen, B.; Tardy, C.; Bailly, C.; Colson, P.; Houssier, C.; Kumar, A.; Boykin, D. W.; Wilson, W. D. *Biopolymers* **2002**, *63*, 281–297. (e) Lacy, E. R.; Le, N. M.; Price, C. A.; Lee, M.; Wilson, W. D. *J. Am. Chem. Soc.* **2002**, *124*, 2153–2163.  
 (26) Davis, T. M.; Wilson, W. D. *Anal. Biochem.* **2000**, *284*, 348–353.

0.1 M KCl and slowly cooled to room temperature. Compounds were added (0–20  $\mu$ M) and reaction mixtures were then incubated for 1 h at room temperature and loaded on a native 12% acrylamide vertical gel in a 0.5 $\times$  TBE buffer supplemented with 20 mM KCl. The gel was run at 4  $^{\circ}$ C for 6 h, dried, and analyzed with a Phosphorimager. Quadruplex formation by some derivatives is shown by the appearance of a new band of retarded mobility.

**Competition Dialysis Experiments.** Dialysis conditions have been described previously.<sup>27</sup> Briefly, a buffer consisting of 15 mM sodium cacodylate, 10 mM MgCl<sub>2</sub>, and 185 mM NaCl (pH 6.5) was used for all experiments. A portion (400 mL) of the dialysate solution containing 1  $\mu$ M ligand was used for each competition dialysis assay. A volume of 200  $\mu$ L at 75  $\mu$ M monomeric unit (nucleotide, base pair, base triplet, or quartet) of each of the DNA samples was pipeted into a separate Dialyzer unit (Pierce). All 19 dialysis units were then placed in the beaker containing the dialysate solution. The beaker was covered with Parafilm and wrapped in foil, and its contents were allowed to equilibrate with continuous stirring at room temperature (20–22  $^{\circ}$ C) overnight. At the end of the equilibration period, DNA samples were carefully transferred to microfuge tubes and treated with 1% SDS. The ligand concentration in each sample was determined by fluorescence (excitation at 320 nm).

A panel of 19 different nucleic acids structures was used.<sup>27</sup> The TC, GA, and GT triplexes result from the association of two strands of different lengths (13 and 30 nucleotides).<sup>28</sup> The 24GA duplex (sample 5) results from the self-association of a (GA)<sub>12</sub> oligonucleotide. The parallel-stranded duplex (psD, sample 6) results from the association of two AT strands: 5' AAAAAAAAAATAATTTTAAATATT and 5' TTTTTTTTTTATTAATAATTTATAA. The 24 CTG (sample 7) mimics eight repeats of the trinucleotide unit (CTG)<sub>8</sub>. ds26 (sample 11) is a 26-base-long duplex formed with a self-complementary oligonucleotide. 22CT [sample 13, 5' (CCCTAA)<sub>3</sub>CCCT] is an oligonucleotide that mimics the cytosine-rich strand of human telomeres and forms an i-DNA structure, whereas 22AG (sample 14) is an oligonucleotide that mimics the guanine-rich strand of human telomeres: 5'-A-(GGGTA)<sub>3</sub>GGG. 24G20 (T<sub>2</sub>G<sub>20</sub>T<sub>2</sub>, sample 15) may form an intermolecular quadruplex.

**TRAP Assay.** The TRAP reaction<sup>3a</sup> was performed in a 20 mM Tris HCl buffer, pH 8.3, containing 63 mM KCl, 1.5 mM MgCl<sub>2</sub>, 1 mM EDTA, 0.005% Tween 20, 0.1 mg/mL BSA, 50  $\mu$ M dTTP, dGTP, and dATP, 10  $\mu$ M dCTP, 0.1  $\mu$ g of the TS and CX primers, 5 ng of the TN primer, 0.05 ng of the TSNT primer, 2 units of Taq polymerase, 40  $\mu$ Ci/tube  $\alpha$ -dCTP,<sup>32</sup> and 200 ng of A549 CHAPS extracts. After telomerase elongation for 15 min at 30  $^{\circ}$ C, 30 cycles of PCR were performed (94  $^{\circ}$ C for 30 s, 50  $^{\circ}$ C for 30 s, and 72  $^{\circ}$ C for 90 s). Telomerase extension products were then analyzed on a nondenaturing 12% polyacrylamide 1 $\times$  TBE vertical gel (2 h at 400 V).

**Fluorometric Titration.** Fluorescence measurements were performed on a Spex Fluoromax spectrophotometer equipped with a Hamamatsu R928 photomultiplier (PM); the data were corrected for the response of the PM. Each sample was prepared in a 0.01 M HEPES buffer (pH 7.4, containing 0.2 M KCl and 0.15 M NaCl) at a constant dye concentration of 10<sup>-7</sup> M. A temperature of 20  $^{\circ}$ C was kept constant with thermostated cell holders. Oligonucleotide 22AG was heated at 90  $^{\circ}$ C for 5 min in 0.01 M HEPES buffer containing 0.2 M KCl and then cooled in ice in order to favor the intramolecular G4 conformation by kinetic trapping. The 17-bp duplex was renatured following the standard protocol.

**Table 1.** Tetraplex DNA Binding Parameters and Telomerase Inhibition

compound	$\Delta T_m^a$ ( $^{\circ}$ C)	TRAP <sup>b</sup> (IC <sub>50</sub> , $\mu$ M)	G4 band <sup>c</sup> Tr2/Ox-1T (%)	$\lambda_{max}^{Fd}$ (nm)
BOQ1	28	0.13	31/76	462
MMQ1	11.5	0.3	7/21	424
MOQ1	12.5	0.5	21/50	nd <sup>e</sup>
MOQ2	10	0.9	nd	462
MOQ0	0	>10	1/0	nd <sup>e</sup>

<sup>a</sup> Stabilization of the F21T oligonucleotide (0.2  $\mu$ M) measured by FRET, for a dye concentration of 1  $\mu$ M in a 10 mM sodium cacodylate buffer, pH 7.2, containing 0.1 M LiCl. The  $T_m$  of the DNA alone was 44  $^{\circ}$ C, and the heating rate in the experiments was 1  $^{\circ}$ C/min. <sup>b</sup> IC<sub>50</sub> against telomerase. <sup>c</sup> Accelerated assembly of G-quadruplexes, as shown by nondenaturing polyacrylamide gel electrophoresis. The percentage shown corresponds to the fraction of radioactivity whose migration corresponds to the quadruplex species formed in the presence of 20  $\mu$ M ligand. The first number corresponds to the results obtained with the Tr2 oligonucleotide; the second number, with the Ox-1T oligomer. <sup>d</sup> Position of fluorescence emission maximum. <sup>e</sup> Not determined.

## Results

**FRET Melting Experiments.** Fluorescence can be used to probe the secondary structure of a quadruplex-forming oligodeoxynucleotide<sup>24</sup> in a manner related to “molecular beacons”.<sup>29</sup> The melting of the G-quadruplex is monitored in the presence of putative G-quadruplex-binding molecules by measuring the fluorescence emission of the donor. A quadruplex-specific ligand should increase the apparent melting temperature ( $T_m$ ) of the F21T quadruplex (5' Fluo-GGGTTAGGGTTAGGGTTAGGG-3'-Tamra), displacing the equilibrium *single strand*–*quadruplex* to the right. This is a qualitative but rapid and convenient initial method to identify promising G4 ligands.<sup>10i,19,24</sup> A series of monomeric dibenzophenanthroline compounds have previously been shown to increase the melting temperature of the G-quadruplex by 0–19  $^{\circ}$ C at 1  $\mu$ M dye concentration.<sup>19</sup>  $T_m$  increases of 10–12  $^{\circ}$ C were measured with the monomers MOQ1–2 and MMQ1, whereas compound MOQ0, lacking the aminoalkyl side chains, showed no effect (Table 1). BOQ1, at 1  $\mu$ M concentration in the standard fluorescence  $T_m$  assay, gave a +28  $^{\circ}$ C stabilization of the quadruplex and is one of the most potent compounds tested to date in this assay.

**BIAcore Surface Plasmon Resonance Experiments.** A more detailed study of the drug–DNA binding interaction was performed by means of surface plasmon resonance, a powerful technology to monitor molecular reactions in real time with the target immobilized on a sensor chip.<sup>25,30</sup> We have previously used this technology to investigate the binding of a variety of compounds to duplex<sup>25,31</sup> and quadruplex<sup>10m</sup> DNAs. Three oligonucleotides, including the human telomeric tetraplex G4 sequence, were immobilized in different flow cells on the same sensor chip, and a range of compound concentrations were injected to monitor the interactions with DNA. Suitable blank control injections with running buffer were also performed and the resulting sensorgrams were subtracted from the compound sensorgrams to obtain the final concentration-dependent graphs (Figure 2).

The experimental conditions were optimized for each binding reaction so that RU values could be obtained for each sensorgram in the steady-state region. Determination of binding

(27) Alberti, P.; Hoarau, M.; Guittat, L.; Takasugi, M.; Arimondo, P. B.; Lacroix, L.; Mills, M.; Teulade-Fichou, M.-P.; Vigneron, J.-P.; Lehn, J.-M.; Mailliet, P.; Mergny, J.-L. In *Small molecule DNA and RNA binders: from synthesis to nucleic acid complexes*; Demeunynck, M., Bailly, C., Wilson, W. D., Eds.; Wiley VCH: in press.  
(28) Mills, M.; Arimondo, P.; Lacroix, L.; Garestier, T.; Hélène, C.; Klump, H. H.; Mergny, J.-L. *J. Mol. Biol.* **1999**, *291*, 1035–1054.

(29) Tyagi, S.; Kramer, F. R. *Nat. Biotechnol.* **1996**, *14*, 303–308.

(30) Malmqvist, M. *Nature* **1993**, *361*, 186–187.

(31) Carrasco, C.; Facompré, M.; Chisholm, J. D.; Van Vranken, D. L.; Wilson, W. D.; Bailly, C. *Nucleic Acids Res.* **2002**, *30*, 1774–1781.

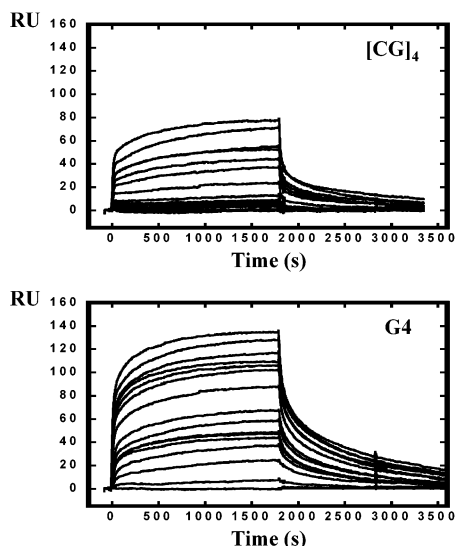


**Figure 2.** SPR sensorgrams for binding of BOQ1 to the immobilized duplex (CG)<sub>4</sub> (upper panel) and the tetraplex [AG<sub>3</sub>(TTAG<sub>3</sub>)<sub>3</sub>] (lower curve) in HBS-EP/KCl buffer at 25 °C. The concentration of the unbound ligand in the flow solution varies from 1 nM in the bottom curve to 10 μM in the top curve in each panel.

**Table 2.** Binding Constants Determined by SPR<sup>a</sup>

compound	sequence	$K_{eq}$ (M <sup>-1</sup> )	$n$
BOQ1	[AATT]	$1.1 \times 10^6$	2
	[GC] <sub>4</sub>	$1.5 \times 10^6$	2
	G4	$1.2 \times 10^7$	2
MOQ2	[AATT]	$1.1 \times 10^6$	1
	[GC] <sub>4</sub>	$1.9 \times 10^6$	1–2
	G4	$1.4 \times 10^6$	2
MMQ1	[AATT]	$4.7 \times 10^5$	3
	[GC] <sub>4</sub>	$4.1 \times 10^5$	4–5
	G4	$8.6 \times 10^5$	4

<sup>a</sup> Experiments were performed at 20 °C in HBS-EP buffer containing 0.2 M KCl. The 5'-biotin oligonucleotide sequences used are d(C-GAATTCGTCTCCGAATTCG), d(CGCGCGCTTTTCGCGCGCG), and d([AG<sub>3</sub>(TTAG<sub>3</sub>)<sub>3</sub>), designated [AATT], [GC]<sub>4</sub>, and G4, respectively.

constants from this experimental region eliminates mass transport-associated problems with the surface. An important parameter that arises naturally from the RU at saturation in SPR experiments is the binding stoichiometry, represented by the  $n$  values in Table 2. During the SPR titration, the increase of RU values is directly proportional to the amount of drug bound to DNA molecules immobilized on the sensor chip.<sup>26</sup> The number of drug molecules interacting with the DNA target can be experimentally determined for each sequence. As indicated in Table 2, the telomeric G4 sequence was found to bind two molecules of BOQ1 and MOQ2. The SPR results were converted to Scatchard plots (Figure 3) and affinity constants were determined by linear fitting. Fitting of direct,  $r$  versus  $C_{free}$ , plots with standard equations presented in the Materials and Methods section gave similar results (not shown). The binding plots shown in Figure 3 point to a highly preferential binding of BOQ1 to the telomeric tetraplex G4 sequence. The monomeric compound MOQ2 binds more weakly to the quadruplex and it has similar affinities for the quadruplex and the duplex sequences.

The quantitative SPR results summarized in Table 2 provide strong evidence for a greater binding affinity of BOQ1 for the human telomeric tetraplex structure compared to the duplex.

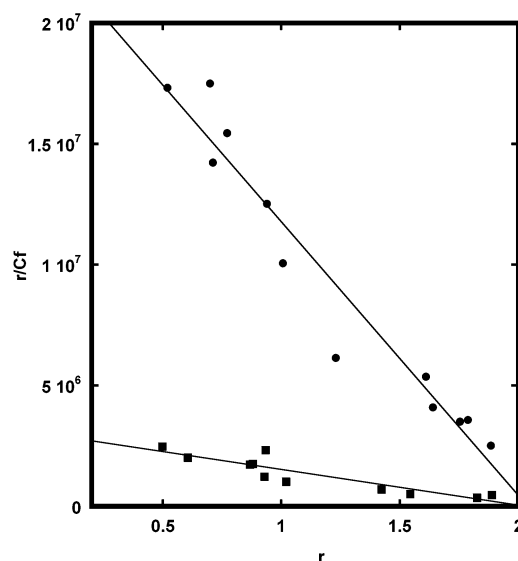


**Figure 3.** Scatchard binding plots ( $r/C_{free}$  vs  $r$ ) used to determine the affinity constants for BOQ1 (●) and MOQ2 (■) complexed with the tetraplex [AG<sub>3</sub>(TTAG<sub>3</sub>)<sub>3</sub>]. To construct these plots, RU values from the steady-state region of the SPR sensorgrams presented in Figure 2 were converted to  $r$  (moles of drug bound/moles of DNA hairpin) at each compound concentration in the flow solution. The lines in the figures are linear least-squares fits to the data with a model for two equivalent binding sites on the tetraplex.  $K$  and stoichiometry values determined in this manner are collected in Table 2.

The equilibrium binding constant of BOQ1 for the two double-stranded sequences [AATT] and [GC]<sub>4</sub> is about 10 times weaker than with the tetraplex. In sharp contrast, compound MOQ2 interacts with the duplexes and the tetraplex with roughly the same affinity, and therefore it must be considered as nonselective under these conditions. The third compound used in the SPR study, MMQ1 with the two aromatic nitrogens on the opposite side of the pentacyclic planar chromophore, presents a modest selectivity for the tetraplex, with a binding constant to the G4 structure about 2 times higher than the equilibrium constants measured with the duplexes (Table 2). This compound is also less selective than BOQ1 and its binding affinity for the telomeric sequence is 1 order of magnitude lower than that of BOQ1. In other words, linking of the MOQ subunits to give the macrocycle BOQ1 provides a compound with considerably improved affinity and selectivity for the quadruplex DNA sequence.

**Fluorescence Spectroscopic Studies.** The interaction of these compounds with G4 DNA was also evaluated by monitoring the spectroscopic properties of these molecules in the presence or absence of a DNA quadruplex. Quinacridines are strongly fluorescent compounds,<sup>16,17</sup> a property that is particularly useful for performing quantitative titrations. Although BOQ1 has a quantum yield that is lower than that of the monomeric derivatives (MOQ2, MMQ1) as expected from a stacked dimeric structure,<sup>16</sup> the quantum yield is sufficient for quantitative titrations. Binding of BOQ1 and MOQ2 to G4 DNA was monitored by recording the fluorescence variation induced by addition of gradual quantities of the 22AG oligonucleotide. Titrations were performed in triplicate at high salt concentration in order to stabilize the quadruplex and to reproduce the experimental conditions used for SPR measurements. Finally, the spectral variations were analyzed by a nonlinear least-squares fitting procedure.<sup>32</sup>

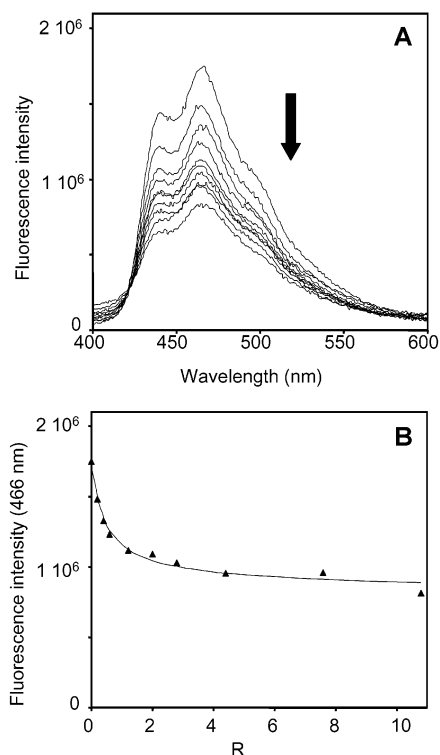


**Figure 4.** (A) Fluorescence spectra of BOQ1 (0.1  $\mu\text{M}$ ;  $\lambda_{\text{exc}}$  316 nm) recorded at increasing concentration of oligonucleotide 22A. (B) Experimental ( $\blacktriangle$ ) and calculated titration curve obtained for the 1:2 stoichiometry;  $R$  = DNA/ligand molar ratio.

A strong quenching (50%) of the fluorescence of BOQ1 was observed upon addition of increasing concentration of the human G4 sequence (Figure 4A). These variations in the emission intensity reflect strong interactions between the macrocycle and the quadruplex. An isoemissive point at 421 nm supports the existence of only two species in equilibrium. The fitting curve (Figure 4B) indicates the formation of a 2:1 complex (two ligands for one G4) with two closely equivalent binding sites, as also observed in the SPR experiments (Figure 3). Calculation of the affinity constant from the curve gave a value of  $(1.0 \pm 0.3) \times 10^7 \text{ M}^{-1}$  per binding site, which also is in the same range as that determined by SPR (see Table 2). The rather large uncertainty of the  $K$  is due to the low concentration of ligand used for the titration that magnifies the problem of adsorption of the dye on the quartz cuvette.<sup>19</sup> Conversely, the addition of a 17-bp duplex to BOQ1 under the same conditions resulted in only a slight decrease of the fluorescence. The variation of the signal was not sufficient to allow a quantitative analysis, but the comparison with the experiment of Figure 4 clearly demonstrates the preferential binding of the macrocycle to the G4 DNA structure. The selective binding of BOQ1 as exhibited by the fluorescence measurements is fully in line with the results obtained from the SPR measurements.

Titration of MOQ2 with the quadruplex DNA caused a large decrease in fluorescence intensity (90%, Figure 5A) with an isoemissive point at 420 nm. The fitting of the experimental data demonstrated the existence of two equivalent binding sites of high affinity [ $K = 3.4 \pm 0.3 \times 10^6 \text{ M}^{-1}$ ] (Figure 5B). Although this value is significantly lower than that measured

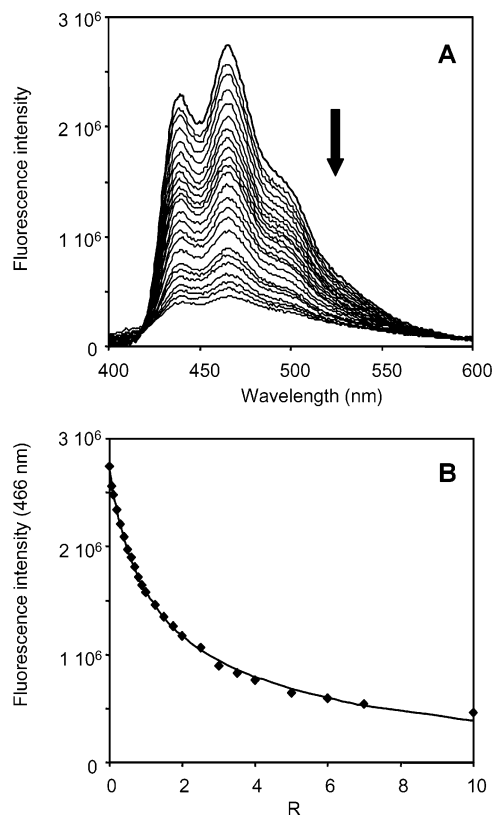


**Figure 5.** (A) Fluorescence spectra of MOQ2 (0.1  $\mu\text{M}$ ;  $\lambda_{\text{exc}}$  360 nm) recorded at increasing concentration of oligonucleotide 22A;  $r$  = DNA/ligand molar ratio. (B) Experimental ( $\blacklozenge$ ) and calculated titration curves obtained for the 1:2 stoichiometry.

for the macrocycle, the difference in the affinities of the two compounds ( $K_{\text{BOQ1}}/K_{\text{MOQ2}} = 2.8$ ) was not so pronounced as that observed by both the SPR measurements ( $K_{\text{BOQ1}}/K_{\text{MOQ2}} = 8.6$ ) and the dialysis experiments (see below). These differences are probably due to the difficulty of determining the very high binding constants of BOQ1 with its lower quantum yield and smaller fluorescence changes on titration with DNA. Altogether, these results point to the higher sensitivity of the SPR and dialysis methods for this system as well as the importance of employing various techniques to improve the precision of parameter estimates.

**Ligand-Mediated Induction of G4 DNA.** The ability of the dibenzophenanthroline to promote intermolecular G4 DNA formation was investigated in an electrophoresis test.<sup>10e</sup> The Tr2 and Ox-1T oligonucleotides were incubated under conditions where little quadruplex structure is obtained in the absence of G4 ligands (20 °C in a 100 mM KCl buffer). Adding increasing amounts of MOQ1, MMQ1, or BOQ1 (from 1 to 20  $\mu\text{M}$ ) to the Tr2 or Ox-1T oligonucleotides led to the progressive appearance of a new band of slower mobility, corresponding to the formation of a bimolecular quadruplex structure.<sup>10e</sup> This is illustrated at the top of Figure 6 and it can be seen that only one new band is obtained on addition of the ligand. Similar results were obtained for the other compounds. The quantification of the gels is shown in the lower part of Figure 6. As expected from their sequences, both oligonucleotides are prone to quadruplex formation. BOQ1 efficiently promotes intermolecular quadruplex formation. Up to 76% of the Ox-1T oligonucleotide was converted into a quadruplex (Figure 6B).

(32) Binstead, R. A.; Zuberbüler, A. D. *Specfit version 2.10*; Spectrum Software Associates: Chapel Hill, NC, 1993.

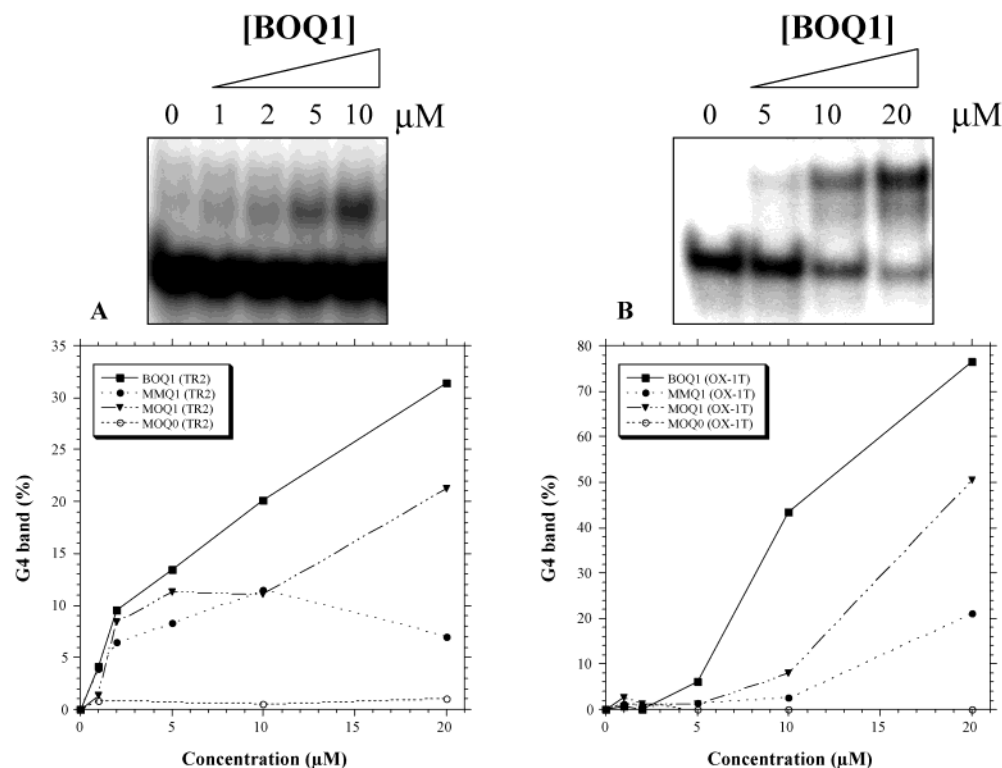


**Figure 6.** Drug-induced formation of intermolecular quadruplex DNA. The graphs show the G4 induction with (A) the Tr2 oligonucleotide and (B) the Ox-1T sequence. Note the differences in y-axis between the two graphs. Examples of representative nondenaturing gels are shown at the top of each panel for BOQ1. Over 20 independent gels were performed to quantify the extent of quadruplex induction. (■) BOQ1; (▼) MOQ1; (●) MMQ1; (○) MOQ0.

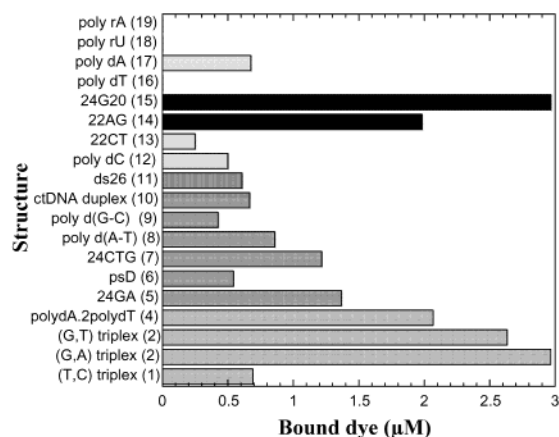


**Figure 7.** Competition dialysis experiments with BOQ1. The amount of drug bound to the various nucleic acid structures (Table 3) is shown as a bar graph. The free ligand concentration in the experiment was 1 μM, and the total concentration of each nucleic acid conformational form was 75 μM (expressed in nucleotides, base pairs, triplet, or tetrad<sup>33</sup>). The stronger binding to tetraplex relative to duplex sequences is easily seen in the comparison (samples 14 and 15, solid bars). The compounds also bind relatively well to several triplex DNA sequences (samples 2–4, dotted bars).

In contrast, MOQ0, which lacks the lateral aminoalkyl side chain, gave very little of the retarded band. These observations are in good agreement with the G4-stabilizing effects shown by other methods; the ligands that have significant G4 interactions efficiently promote quadruplex formation. The larger effects of the compounds on the Ox-1T oligonucleotide are due to the greater stability of the G4 structure with this sequence.

**Competition Dialysis Experiments.** The sequence and structural selectivity of various different DNA binding agents has been previously explored by use of a thermodynamically

rigorous competition dialysis procedure introduced by Ren and Chaires.<sup>33</sup> In this method, different nucleic acid structures are dialyzed against a common ligand solution. More ligand accumulates in the dialysis tube containing the structural form with the highest ligand binding affinity. This is a simple method to evaluate specificity toward quadruplexes.<sup>27,33</sup> As shown in Figure 7, BOQ1 displays a strong preference for binding to G-quadruplexes, with a slight preference for the parallel tetraplex structure 24G20. BOQ1 binds strongly to 22AG, which corresponds to the human telomeric G-rich motif, while little or no binding to single strands is observed. The affinity for double strands is lower than the affinity for quadruplexes or triplexes. Overall, these studies confirm that BOQ1 binds preferentially to quadruplexes as compared to single- or double-stranded sequences. The compound also binds reasonably well to the triple-stranded sequences, though the interaction with the pyrimidine (T,C) motif is weak compared to that with the purine (G,T) and (G,A) motifs. These equilibrium dialysis measurements nicely complement the SPR data to indicate that BOQ1 exhibits a significant preference for the tetraplexes as opposed to the duplexes.

**Telomerase Inhibition.** Once G4 stabilization and induction was established for BOQ1, it was important to test whether the molecule inhibits telomerase activity in a modified TRAP assay.<sup>10i,34</sup> The assay clearly shows that BOQ1 is a potent inhibitor of telomerase with activity in the submicromolar range (IC<sub>50</sub> = 0.13 μM, Figure 8). The compound is a weaker inhibitor of Taq polymerization as shown by the disappearance of the

(33) (a) Ren, J. S.; Chaires, J. B. *Biochemistry* **1999**, *38*, 16067–16075. (b) Ren, J.; Chaires, J. B. *Methods Enzymol.* **2001**, *340*, 99–108. (c) Ren, J.; Chaires, J. B. *J. Am. Chem. Soc.* **2000**, *122*, 424–425.  
(34) Krupp, G.; Kuhne, K.; Tamm, S.; Klapper, W.; Heidorn, K.; Rott, A.; Parwaresch, R. *Nucleic Acids Res.* **1997**, *25*, 919–921.

**Table 3:** Nucleic Acids Structures Used for Dialysis<sup>a</sup>

no.	name	type <sup>b</sup> (length)	structure	$\epsilon^c$ (M <sup>-1</sup> cm <sup>-1</sup> )
1	TC triplex	oligos (30 + 13)	triplex	377 700
2	GA triplex	oligos (30 + 13)	triplex	425 000
3	GT triplex	oligos (30 + 13)	triplex	399 200
4	poly(dA)·2poly(dT)	poly	triplex	17 200
5	GA duplex	oligo (24)	"duplex" <sup>b</sup>	281 500
6	ps duplex	oligos (30 + 30)	"duplex" <sup>b</sup>	530 700
7	24CTG	oligo (24)	"duplex" <sup>b</sup>	194 900
8	poly[d(A-T)]	poly	duplex	13 200
9	poly[d(G-C)]	poly	duplex	16 800
10	CT DNA	poly	duplex	12 820
11	ds 26	oligo (26)	duplex	253 200
12	poly(dC)	poly	i-DNA	7400
13	22CT	oligo (22)	ss/i-DNA <sup>c</sup>	193 700
14	22AG	oligo (22)	G4	228 500
15	24G20	oligo (24)	G4	235 600
16	poly(dT)	poly	single-str	8520
17	poly(dA)	poly	single-str	8600
18	poly(rU)	poly	single-str	9350
19	poly(rA)	poly	single-str	9800

<sup>a</sup> Nineteen different nucleic acid structures were used (samples labeled 1–19, left column). <sup>b</sup> poly = polynucleotide; oligo = oligonucleotide; oligos = structure formed by the association of two different oligonucleotides. The length of the oligomer(s) is shown within parentheses. Polynucleotides are > 100 bases-long. <sup>c</sup> For polynucleotides, the extinction coefficient (in italic type) is given per base [for single strands and poly(dC)] base pair (for duplexes) or base triplets (for triplexes) as suggested by Ren and Chaires.<sup>33</sup> For oligonucleotides, the extinction coefficient corresponds to the oligonucleotide or the sum of the two different oligonucleotides (TC, GA, and GT triplexes and parallel duplex) for the unfolded species, according to the manufacturer (Eurogentec, Belgium). <sup>d</sup> These three duplexes involve the formation of nonclassical base pairs. <sup>e</sup> 22CT may form an i-DNA structure but is mainly single-stranded at 20 °C.

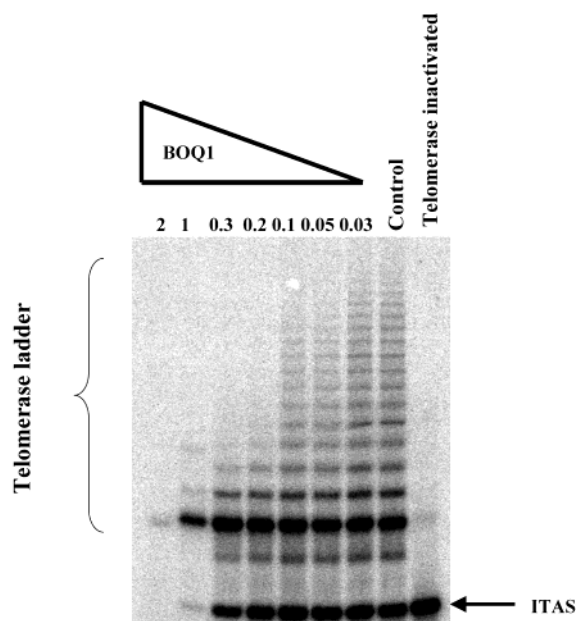


**Figure 8.** Telomerase inhibition by BOQ1. The gel shows the effect of increasing concentrations of compound BOQ1 on telomerase activity. High concentrations (3–10  $\mu$ M) of the macrocycle lead to the disappearance of all PCR products. At intermediate concentrations (0.2–0.3  $\mu$ M) only the telomere ladder is affected. The position of the internal standard (ITAS) is indicated. Results for a heat-inactivated extract are shown in the right lane.

internal PCR standard (ITAS) band around 1  $\mu$ M. The IC<sub>50</sub> for the internal standard was determined to be 0.3  $\mu$ M for Taq, significantly higher than the IC<sub>50</sub> against telomerase.

## Discussion

As described in the Introduction, in addition to its well-known roles in protecting the ends of chromosomal DNA, telomere

DNA with its associated proteins is now recognized to play a variety of important cellular roles. It is also clear that the telomerase enzyme that produces telomere DNA is active in many cancer cells as well as in several disease-causing parasitic microorganisms. Inhibition of this enzyme, which is inactive in most normal human cells, could thus provide a selective therapeutic strategy. Telomere DNA can form a number of interesting structures, including quadruplexes composed of G4 tetrads.<sup>2</sup> This structure is readily formed in vitro in the presence of cations such as K<sup>+</sup> and Na<sup>+</sup> by G-rich strands such as the human -(TTAGGG)<sub>n</sub>- telomere repeat. Several studies now indicate that driving the telomere G-strand into a quadruplex can result in inhibition of the telomerase enzyme.<sup>7,10</sup> Identification of classes of compounds that can selectively stabilize G-quadruplexes is an active research area that has importance for therapeutic development as well as for development of a better understanding of DNA interactions.<sup>10</sup>

Quadruplex DNA structure polymorphism leads to uncertainties about the binding mode of compounds that target the quadruplex, making the rational design of G4-directed small molecules difficult. Although a relatively small number of molecules are currently known that selectively target telomere quadruplexes, analysis of their structures and consideration of macrocycle–DNA interactions strongly suggested that macrocycles could selectively target quadruplexes. Such compounds are more similar in size to the G-quartet than classical intercalators (Figure 1). As a first step in the analysis of the interaction of macrocyclic compounds with quadruplexes, the ability of BOQ1 to raise the T<sub>m</sub> of a labeled quadruplex was evaluated in a FRET-based assay. FRET melting experiments have been extensively validated for rapid, qualitative identification of compounds as G4 binding agents.<sup>10i,j,19,24</sup> In the FRET assay, the charged monomers in Figure 1 stabilize a quadruplex based on the human telomere sequence by 10–12 °C. The macrocycle BOQ1, which is directly related to the monomer structures, stabilizes the DNA by a much larger 28 °C. This result clearly shows that the macrocycle is one of the strongest G4-stabilizing agents discovered to date.

Multiple DNA competition dialysis is a method, recently developed by the Chaires' laboratory,<sup>33</sup> to compare binding of compounds to a broad panel of DNAs and RNAs for rapid evaluation of binding sequence and structural specificity. A strong interaction of the macrocycle with G4 structures and weak interaction with all single-stranded and duplex DNAs is easily visualized from the results of this assay (Figure 7). Binding to duplex natural DNAs as well as synthetic polymers composed completely of either AT or GC is significantly weaker than for the two G4 structures included in the assay. The macrocycle also binds strongly to some triplex DNAs including the T·A·T triplex where the bases are completely different than with the G4 quadruplexes. Since triplex DNA structures are not major components of cellular DNA, triplex interactions should not interfere with G4 binding in biological systems. These results with DNAs of quite different base composition suggest that the stacking ability, rather than direct base interactions, of the macrocycle is the key feature responsible for its selectivity with quadruplex and triplex DNA structures.

The binding affinity and stoichiometry of the macrocycle to quadruplex and duplex DNAs has been evaluated with more detailed studies by biosensor-SPR and fluorescence titration



methods. Values for stoichiometry arise naturally from the SPR results through analysis of the maximum RU values observed as saturating concentrations of the compound with the target DNA sequence are approached. The SPR results indicate two essentially equivalent binding sites for the macrocycle with quadruplexes based on the human telomere (Figure 3), and fitting of fluorescence titration results also agrees with two sites per quadruplex. Both SPR and fluorescence results predict a BOQ1 binding constant of  $10^7 \text{ M}^{-1}$  or larger for the human quadruplex sequence. Binding constants for duplex sequences are at least 10 times lower as suggested by the competition dialysis comparisons. Binding constants for the monomer control compounds are around a factor of 10 lower for the human G4 sequence than for BOQ1 (Figure 3). The monomers and the macrocycle have similar binding constants with duplex DNAs, however, and the macrocycle thus has much greater quadruplex binding specificity.

The two strong and equivalent binding sites for the macrocycle are consistent with the quadruplex tetrad stack, with two ends available for stacking interactions. The observation is unusual for G4 binding compounds, however. Most compounds discovered to date that target quadruplexes either stack on only one end of the structure or stack much more strongly on one end than the other.<sup>10</sup> NMR studies of interstrand quadruplexes based on the human (TTAGGG)<sub>n</sub> sequence, however, indicate that a methylacridinium compound can also stack well at both ends of the G4 structure.<sup>10i</sup> Similar studies with perylene-based G4 binding compounds indicate that they prefer to stack at the GT quadruplex terminus.<sup>10p,15c</sup> These results suggest that both ends of the quadruplex are potential sites for stacking of large aromatic cations and the macrocycle is able to bind simultaneously and strongly to both. This may be a feature of the type and shape of ring system present in the compounds in Figure 1, since the monomer compounds bind more weakly to the quadruplex but also appear to have two equivalent binding sites (see Figure 3, for example).

It should be emphasized that BOQ1 is a flexible molecule that may adopt various conformations upon binding and the structure of the compound in the complex is important for drug design. BOQ1 conformations can vary from an open flat form to a semiclosed structure (Figure 1). Although structural analysis by NMR or X-ray is required to determine the conformation of BOQ1 in the G4 complex, it is interesting to consider the likely general structure. The large planar surface of the G4 tetrad suggests that an optimum complex could form by end stacking of the macrocycle in its open flat conformation. The potential for this type of complex was part of our original rationale for analysis of macrocycle–G4 interactions. Thus, the dimeric structure of the macrocycle can increase G4 affinity relative to the monomers in Figure 1 through enhanced stacking/hydro-

phobic interactions. It should also be noted that the semiclosed conformation of BOQ1, which has the two quinacridine units held in a parallel orientation (Figure 1), is similar to the dimers formed by minor-groove binders such as distamycin and related derivatives. Therefore, possible binding of the semiclosed form of BOQ1 in the grooves of the G4 DNA should also be considered as an alternative or additional possibility to the end-stacking mode observed for most planar aromatic compounds. It would appear then that molecular flexibility may play a key role in the G4 binding specificity of BOQ1. It is possible that the flexibility of the macrocycle as well as the internal mobility of G4 DNA allows the two partners to assemble in an unusual complex structure in which the specificity might originate.

In summary, a variety of experiments all indicate that the macrocycle BOQ1 binds significantly more strongly to quadruplexes than to duplexes and more strongly to the quadruplex than the monomer compounds. Although this is of fundamental interest for understanding molecular interactions of quadruplexes, design of G4 targeting compounds is of particular interest for their potential to inhibit telomerase and cancer progression. A number of small ligands have been discovered to inhibit the function of telomerase by stabilizing G4 DNA structures.<sup>4,7,10</sup> These ligands appear to function by locking a telomeric G-strand into a folded conformation that cannot be extended by telomerase. BOQ1 was evaluated in a TRAP assay to determine its ability, relative to other compounds, to inhibit telomerase. The excellent IC<sub>50</sub> for telomerase inhibition by BOQ1 (0.13  $\mu\text{M}$ ) is in the range expected from its binding constant ( $K > 10^7 \text{ M}^{-1}$ ). It is clear that macrocycles represent an exciting new development opportunity for targeting DNA quadruplexes.

**Acknowledgment.** This paper is dedicated to the memory of Professor Claude Hélène. This work was supported by grants (to C.B.) from INSERM and the Ligue Nationale Contre le Cancer (Equipe labellisée La Ligue); (to J.L.M.) from CNRS, INSERM, and the Association pour la Recherche sur le Cancer (ARC Grant 4321); and (to W.D.W.) from the National Institutes of Health and the Gates Foundation. W.D.W. was the recipient of an INSERM “Poste Orange” Senior Scientist Fellowship for research in the Bailly Laboratory, ICRL, Lille, France. This research has been supported by a Marie Curie Fellowship (to C.C.) of the European Community Program “Improving Human Research Potential and the Socio-economic Knowledge Base” under Contract HPMFCT-2000-00701. C.B. thanks the IMPRT for access to the BIAcore 3000 instrumentation, and J.L.M. thanks M. Hoarau, L. Lacroix, P. Arimondo, and C. Hélène (Muséum, Paris) for helpful discussions.

JA021299J